Memoirs of the Faculty of Engineering, Okayama University, Vol. 33, No.1, pp. 5-17, November 1998

Rigid-Plastic Deformation of Inhomogeneous Material with Elliptic Inclusions Sliding along Boundary

Takeji ABE*, Ryuji NAMIKOSHI**, Noriyuki NAGAYAMA***
and Yasuju TAKANO****

(Received October 9 , 1998)

The influence of the slip between the inclusion and the matrix during the plastic deformation of inhomogeneous material with elliptic inclusions is investigated. The material is assumed to be rigid-plastic. The boundary slip region is modeled by assuming lower yield stress for the thin boundary region than those of the inclusion and the matrix. The rigid-plastic finite element method is used for the numerical calculation under the plane strain condition. The effects of the aspect ratio of the inclusion, the yield stress of the boundary region, and the volume fraction of the inclusion on the deformation mode are studied. The patterns of the strain concentration and the averaged flow stress of the inhomogeneous material are also discussed. The results may be helpful for understanding creep or superplastic deformation of metals with inclusions.

Key words : *Plasticity, Composite Material, Sliding Inclusions, Rigid-Plastic Deformation, Finite Element Method*

1. INTRODUCTION

Engineering materials are usually inhomogeneous. It is important to study the plastic deformation of inhomogeneous material with inclusions as a representative example of inhomogeneous materials[(1)-(11)]. When the inhomogeneous material with inclusions is deformed plastically, the slip between the inclusion and the matrix is one of the most important factors for the deformation of the material. Although the plastic deformation of inhomogeneous material with inclusions has been studied in several papers, sliding between the inclusion and the matrix has scarcely been considered[(5)(6)]. Figure 1 shows an example of micrograph of plastic deformation of metallic material with inclusions (high-carbon steel) taken by Oyane and Sekiguchi[(12)]. It is seen that slip bands are often formed through the boundary region between the inclusion and the matrix.

On the other hand, elastic inclusion problem has been treated successfully in the micromechanics[(13)-(16)]. The plastic

* Department of Mechanical Engineering and Cooperative Research Center, Okayama University, 3-1-1, Tsushima-Naka, Okayama, 700, Japan
** Shikoku Instrumentation Co., Ltd., 777, Oosa-cho, Zentsuji-city, Kagawa, 765
*** Industrial Technology Center of Okayama Prefecture, Haga, Okayama, 701
**** Kobe Steel, Ltd., Chuou-ku, Kobe, 651

inclusion problem, however, may be solved only numerically and the role of computational micromechanics is important. In the present paper, the effects of the slip between the elliptic inclusion and the matrix on the plastic deformation behaviour of the inhomogeneous material are investigated. The rigid-plastic finite element method (FEM) is used for the numerical analysis, which is based on the upper bound theory of plasticity. Rigid-perfectly plastic solution is important not only for plastic deformation problems with large strain, but also for creep deformation problems through the plastic analogy in the creep analysis.

The effects of the aspect ratio of the inclusion, the yield stress of the boundary region, and the volume fraction of the inclusion and the boundary region, are examined. The patterns of the heavily deformed region produced along the boundary region and the averaged flow stress of the inhomogeneous material are also investigated.

2. METHOD OF CALCULATION

2. 1 Analysis

The rigid-plastic finite element method[17], which is widely used in the analysis of metal working processes, is used for the numerical calculation under the plane strain condition. Namely, it is known from the variational principle that the following functional takes the minimum value for the correct velocity field.

$$\Phi = \int \sigma_{eq}\, \dot{\varepsilon}_{eq}\, dV + \frac{1}{2}\beta \int \dot{\varepsilon}_v^2\, dV - \int \boldsymbol{T}\boldsymbol{u}\, dS \tag{1}$$

σ_{eq} is the equivalent stress and we assume σ_{eq}=Y in the plastic region, where Y is the yield stress. $\dot{\boldsymbol{\varepsilon}}_{eq} = (2/3\ \dot{\boldsymbol{\varepsilon}}^{\mathrm{T}}\ \dot{\boldsymbol{\varepsilon}})^{1/2}$ is the equivalent strain rate, **T** is the force given at the surface S_t of the body, and **u** is the admissible velocity field. $\dot{\boldsymbol{\varepsilon}}_v$ is the volumetric strain rate, and $\dot{\boldsymbol{\varepsilon}}_v = 0$ expresses the condition of incompressibility. β is a large coefficient called the penalty number. When the penalty number is sufficiently large, $\dot{\boldsymbol{\varepsilon}}_v$ is negligible at the minimum of the functional Φ, hence the condition of volume constancy is approximately satisfied.

Shimizu et al[18] showed that Eq. (1) can be discretized as follows. For the whole elements we have

$$\sum \frac{\partial \Phi^{(m)}}{\partial u^{(m)}} = 0 \quad , \tag{2}$$

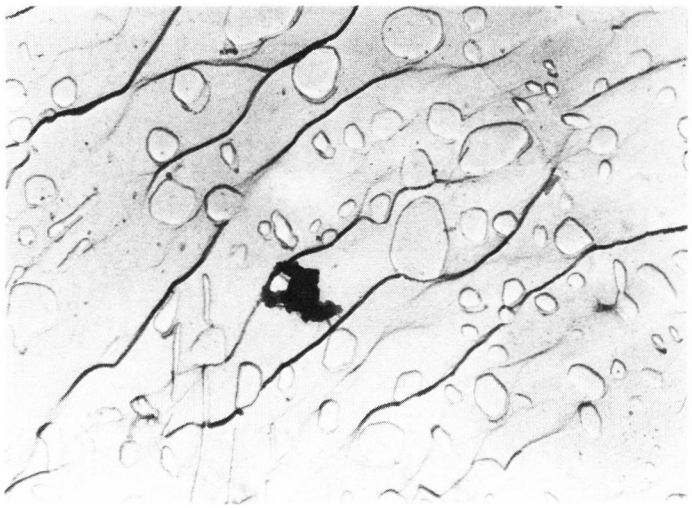

Fig. 1 Example of micrograph of plastic deformation of metal with inclusions (high-carbon steel[11])

where m is the number of elements. Then, the following relations are obtained for respective element

$$\frac{\partial \phi^{(m)}}{\partial u^{(m)}} = (Y\boldsymbol{P}_{n-1} + \beta \boldsymbol{Q})\,\Delta \boldsymbol{u}_n - F + Y\boldsymbol{H}_{n-1} + \beta \boldsymbol{Q} u_{n-1} \tag{3}$$

$$\boldsymbol{P} = \frac{2}{3}\int_v \frac{1}{(\dot{\varepsilon}_{eq})_{n-1}}\left(\boldsymbol{B}^T\boldsymbol{B} - \frac{2\lambda}{3(\dot{\varepsilon}_{eq})_{n-1}^{\,2}}\boldsymbol{b}_{n-1}\boldsymbol{b}_{n-1}^T\right)dV \tag{4}$$

$$\boldsymbol{Q} = \int_v \boldsymbol{B}^T\boldsymbol{C}\boldsymbol{C}^T\boldsymbol{B}\,dV \tag{5}$$

$$\boldsymbol{F} = \int_s \boldsymbol{N}^T\boldsymbol{T}\,dS \tag{6}$$

$$\boldsymbol{H} = \frac{2}{3}\int_v \frac{\boldsymbol{b}_{n-1}}{(\dot{\varepsilon}_{eq})_{n-1}}\,dV \tag{7}$$

$$\boldsymbol{b}_{n-1} = \boldsymbol{B}^T\boldsymbol{B}\,\boldsymbol{u}_{n-1} \tag{8}$$

$$(\dot{\varepsilon}_{eq})_{n-1}^2 = \frac{2}{3}\boldsymbol{u}_{n-1}^T\boldsymbol{B}^T\boldsymbol{B}\boldsymbol{u}_{n-1} \tag{9}$$

$$\dot{\varepsilon} = \boldsymbol{B}\,\boldsymbol{u}\ , \quad \dot{\varepsilon}_v = \dot{\varepsilon}^T\boldsymbol{C}\ , \tag{10}$$

where $\boldsymbol{N}$ is the displacement shape function, $\boldsymbol{B}$ is the strain shape function and $\boldsymbol{C}$ is a coefficient matrix. n is the number of repeated calculations. λ is a parameter ($0 \le \lambda \le 1$). $\lambda = 0$ and $\lambda = 1$ correspond to Gauss–Newton method and Newton–Raphson method in the repeated calculation, respectively. In the following numerical calculation, we assumed $\lambda = 0$, which gives better convergence of numerical solution for inhomogeneous body. Mises yield condition and Levy–Mises flow rule are assumed. In the following consideration, strain–rate is transformed into strain considering a unit time.

2. 2 Model of Material with Inclusions

A plane model of inhomogeneous material with regularly distributed inclusions shown in Fig. 2 (a) and (b)is assumed. Considering the symmetric configuration of the model, the region OACB is used for the numerical calculation. The region OACB is divided into 414 triangular isoparametric elements with 869 nodes[19]. A thin boundary region is assumed between the inclusion and the matrix. All the inclusions, the boundary region and the matrix are supposed to be rigid–plastic. The boundary slip is modeled by assuming lower yield stress for the boundary region than those of the inclusion and the matrix.

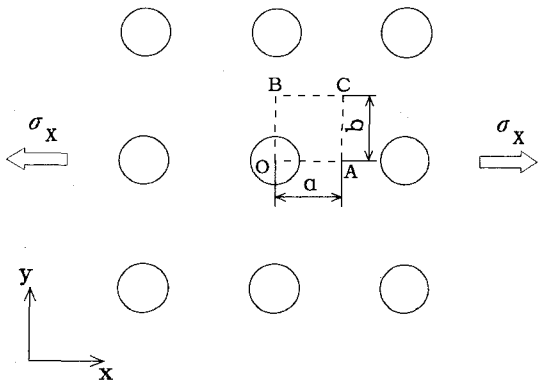

Fig. 2 (a) Plane model of inhomogeneous material with inclusion and soft boundary region

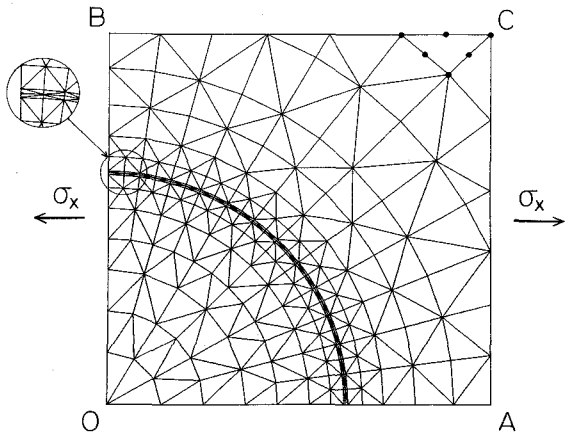

(b) Finite element mesh

2. 3 Characteristic Parameters of Inhomogeneous Material

Several parameters are introduced to define material inhomogeneity quantitatively.

(a) Volume fraction $(V_f)_I$ and $(V_f)_B$

The volume fractions of the inclusion and the boundary region are defined respectively as follows

$$(V_f)_I = V_I / V \quad , \quad (V_f)_B = V_B / V \quad , \tag{11}$$

where V_I, V_B and V are the volumes of the inclusion, the boundary region and the whole material, respectively. In the following numerical calculation, the width of the boundary region of the model is assumed to be 1% of the length of the side OA or OB, unless otherwise stated. Hence, the volume fractions of the boundary region are $(V_f)_B$ = 0.0056, 0.0097 and 0.0125 for the volume fractions of the inclusion $(V_f)_I$ = 0.1, 0.3 and 0.5, respectively.

(b) Aspect ratio R

The aspect ratio of the model material with inclusions shown in Fig. 2 is defined as follows.

$$R = b / a \tag{12}$$

(c) Ratio of yield stress α_I and α_B

The ratios α_I and α_B of yield stress of the inclusion and the boundary region to the yield stress of the matrix, respectively, are expressed as

$$\alpha_I = \sigma_I / \sigma_M \quad , \quad \alpha_B = \sigma_B / \sigma_M \quad , \tag{13}$$

where σ_I, σ_B and σ_M are the yield stresses of the inclusion, the boundary region and the matrix, respectively.

2. 4 Parameters Expressing Deformation Behaviour of Material

In order to express the calculated deformation patterns quantitatively, the following parameters are introduced.

(a) Strain concentration coefficients A_I, A_B and A_M

The strain concentration coefficients were originally defined by Hill[20] in tensorial form. In the present paper, however, the averaged strain concentration coefficients A_I, A_B and A_M of the inclusion, the boundary region and the matrix, respectively, are defined with the averaged equivalent plastic strain as follows.

$$(\overline{\varepsilon_{eq}})_I = A_I \, \tilde{\varepsilon}_{eq} \, , \quad (\overline{\varepsilon_{eq}})_B = A_B \, \tilde{\varepsilon}_{eq} \, , \quad (\overline{\varepsilon_{eq}})_M = A_M \, \tilde{\varepsilon}_{eq} \tag{14}$$

$(\overline{\varepsilon_{eq}})_I$, $(\overline{\varepsilon_{eq}})_B$, $(\overline{\varepsilon}_{eq})_M$ and $\tilde{\varepsilon}_{eq}$ are the averaged equivalent plastic strains for respective elements of the inclusion, the boundary region, the matrix and the whole material, respectively. The averaged strain concentration coefficients are useful in describing the averaged behaviour of inclusion, the boundary region and the matrix based on the plastic work. For homogeneous deformation, it is obvious that $A_I = A_B = A_M = 1$.

(b) Parameter χ of strain multiaxiality

The ratio of the averaged equivalent plastic strain $\tilde{\varepsilon}_{eq}$ obtained from the finite element calculation to the applied equivalent plastic strain ε^* is denoted with χ and called as the parameter of strain multiaxiality.

$$\chi = \tilde{\varepsilon}_{eq} / \varepsilon^* \tag{15}$$

This parameter expresses the complexity of the strain distribution, that is, the deviation from homogeneous strain distribution. For the homogeneous material, the distribution of strain is uniform, and hence we have $\chi = 1$.

3. RESULTS OF CALCULATION AND DISCUSSION

The applied strain is assumed to be ε_x = 0.01 in x-direction (ε_y = −0.01 in y-direction). This value, however, is not essential in the calculated results shown below, because they are normalized with respect to ε_x. The effect of boundary slip on the deformation behaviour is studied considering the following two cases.

3. 1 Case of Equal Yield Stress for Inclusion and Matrix

At first, the yield stresses of the inclusions and the matrix are assumed to be equal (α_I = 1.0), while the boundary region has lower yield stress (α_B < 1.0). In order to examine the effect of the boundary slip on the deformation behaviour of inhomogeneous material with inclusion, the strain distribution is calculated for various values of the aspect ratio R and the yield stress ratio α_B of the boundary region.

Figure 3 shows the distribution of the equivalent plastic strain for the cases of α_B = 0.1, 0.9 and R = 1, 3, 5, where the values are normalized with respect to the applied strain ε_x . As is seen from Fig. 3, the equivalent plastic strain is maximum along the boundary region. When the inclusion is circular (R = 1), characteristic deformation bands appear along the boundary region. Deformation bands are formed especially along the boundary when α_B is small. The strain distribution is symmetric with respect to the diagonal line OC for the case of R = 1 under the plane strain condition.

Figure 4 shows the relation between the strain concentration coefficients A_I , A_B , A_M and the aspect ratio R. As shown in Fig. 4 (a), A_I is small for the aspect ratio R between 0.5 and 2.0. This is because deformation bands appear

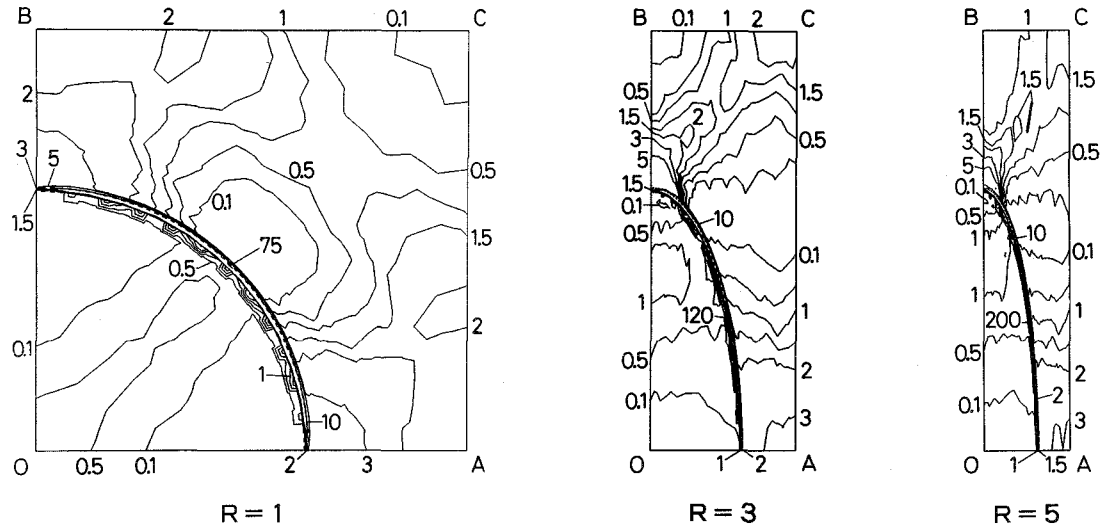

(a) α_B = 0.1

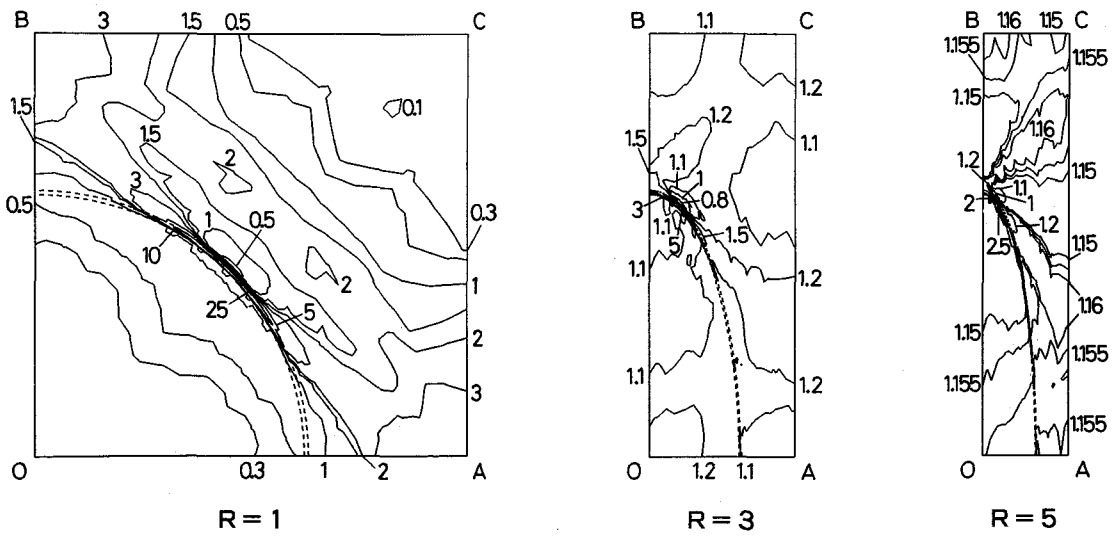

(b) α_B = 0.9

Fig. 3 Distribution of equivalent plastic strain ε_{eq} [$(V_f)_I$ = 0.3, α_I = 1.0, unit : ε_x]

in the matrix for R between 0.5 and 2, and hence the strain of the inclusion becomes small. [As shown in Fig. 4(a), the calculated result under the plane strain condition is logarithmically symmetric with respect to the aspect ratio R = 1. Hence, only the right half side $R \geq 1$ will be shown in the following figures.] As shown in Fig. 4 (b) for the case of α_B = 0.1, the value of A_B is large as R increases from 2, which suggests the slip in the boundary region increases.

Figure 5 shows the relation between the parameter χ of strain multiaxiality and the aspect ratio R. When the yield stress ratio α_B of the boundary region is equal to 0.9 and 0.5, the value of χ is almost close to 1. Meanwhile, when the ratio is small (α_B = 0.1), χ increases with the increase in R, which means the effect of slip at the boundary region becomes large.

Next, we consider the averaged flow stress for the whole material[8][9]. The averaged flow stress of the material and the applied strain are denoted with σ^* and ε^*, respectively. As the external plastic work is equivalent to the internal plastic work, we have

$$\sigma^* \varepsilon^* = (V_f)_I \, \sigma_I(\overline{\varepsilon_{eq}})_I + (V_f)_B \, \sigma_B(\overline{\varepsilon_{eq}})_B + \{ 1-(V_f)_I - (V_f)_B \} \, \sigma_M(\overline{\varepsilon_{eq}})_M \quad . \tag{16}$$

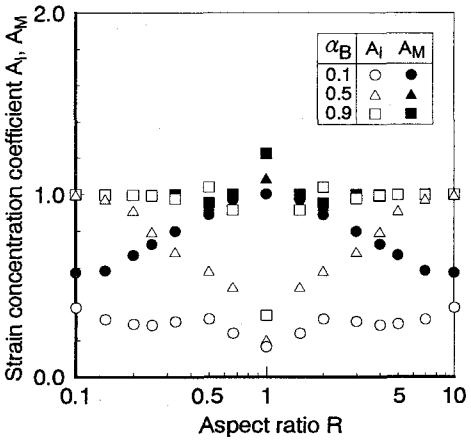

(a) A_I and A_M

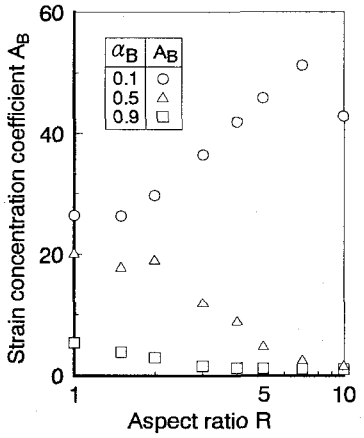

(b) A_B

Fig. 4 Relation between strain concentration coefficients A_I, A_M, A_B and aspect ratio R [$(V_f)_I$ = 0.3 , α_I = 1.0]

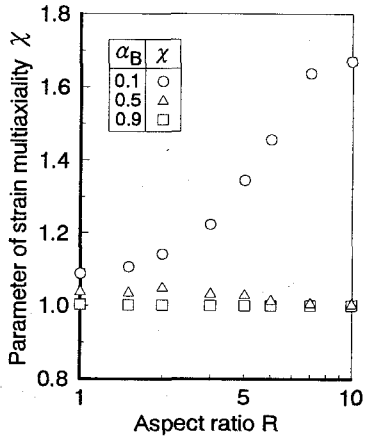

Fig. 5 Relation between parameter χ of strain multiaxiality and aspect ratio R [$(V_f)_I$ = 0.3 , α_I = 1.0]

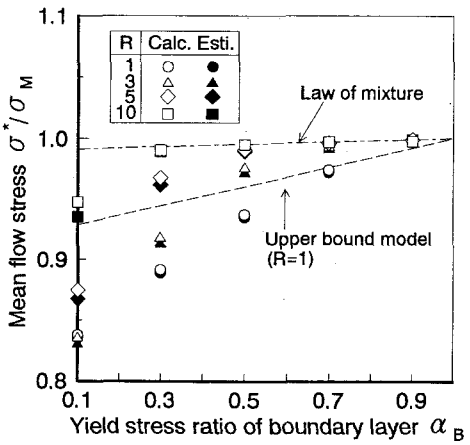

Fig. 6 Relation between averaged flow stress σ^*/σ_M and yield stress ratio α_B of boundary region [$(V_f)_I$ = 0.3 , α_I = 1.0]

Meanwhile, the averaged equivalent plastic strain of the whole material is expressed with the averaged equivalent plastic strains defined in Eq. (14) as follows.

$$\bar{\varepsilon}_{eq} = (V_f)_I(\overline{\varepsilon_{eq}})_I + (V_f)_B(\overline{\varepsilon_{eq}})_B + \{1-(V_f)_I-(V_f)_B\}\sigma_M(\overline{\varepsilon_{eq}})_M \tag{17}$$

Hence, the following relation is obtained from Eqs. (13) - (17).

$$\frac{\sigma^*}{\sigma_M} = \{(\alpha_I-1)A_I(V_f)_I + (\alpha_B-1)A_B(V_f)_B + 1\}\chi \ . \tag{18}$$

The averaged flow stress of the material is given with Eq. (18). When the material deforms uniformly, $A_I=A_B=A_M=1$ and $\chi = 1$. Then, we have

$$\sigma^* = (V_f)_I\,\sigma_I + (V_f)_B\,\sigma_B + \{1-(V_f)_I-(V_f)_B\}\,\sigma_M \tag{19}$$

Eq. (19) is the well-known law of mixture for the composite materials.

Figure 6 shows the relation between the ratio σ^*/σ_M of the averaged flow stress of the whole material to the yield stress of the matrix and the ratio of the yield stress α_B of the boundary region. The alternate dot and dashed line expresses the value obtained from the law of mixture [Eq. (19)]. The open marks of σ^*/σ_M obtained from the calculated nodal force almost coincide with the corresponding solid marks calculated from Eq. (18) using the calculated values of A_I, A_B and χ. The calculated values of σ^*/σ_M are lower than the values obtained from the law of mixtures when the value of α_B is small and R is close to 1. This shows that the averaged flow stress decreases with the formation of deformation bands along the boundary region.

The calculated averaged flow stress shown in Fig. 6 is lower than that expected from the law of mixture. On the other hand, the flow stress is also estimated from a simple velocity field with velocity discontinuity based on the upper bound method in plasticity as follows. The strain distribution for $R = 1$ shown in Fig. 3 is approximated with the velocity field composed of the lines of shear velocity discontinuity inclined 45 degree to the direction of the applied stress, as shown in Fig. 7. Namely, shear deformation is assumed to occur along the lines HIJKH of the velocity discontinuity. In the present model, the thickness of the boundary region is assumed to be 1% of the length $\overline{OA}$ shown in Fig. 2. In order to express the decrease of the flow stress of the boundary region, the yield stress ratio α_B is supposed to decrease along the length of the velocity discontinuity line which passes the thickness of the boundary region. The estimated value is shown with the dashed line in Fig. 6, which still overestimates the calculated results for $R = 1$ (o marks).

It is usually known that fine grains and spherical grain shape are necessary for the superplastic deformation of metallic compounds. The result shown in Fig. 6 may explain the deformation of superplastic metals, where the grain boundary slip and isotropic shape of fine grains are important for the superplastic behaviour.

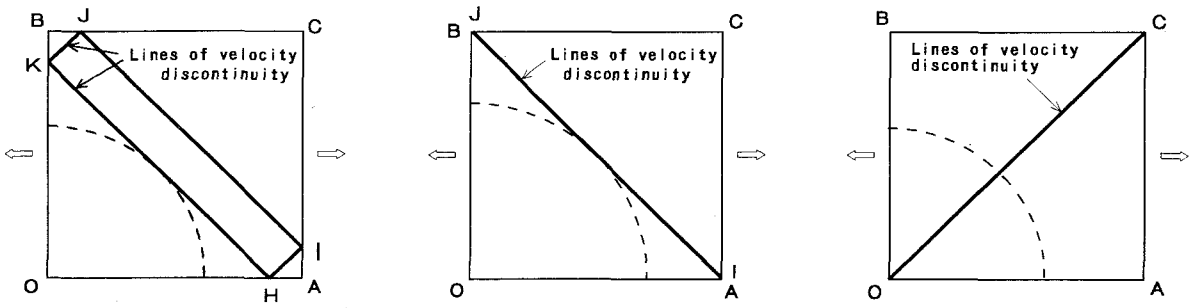

(a) Sliding boundary (Hard inclusion), $(V_f)_I = 0.3$

(b) Sliding boundary (Hard inclusion), $(V_f)_I = 0.4$

(c) Soft inclusion $(V_f)_I = 0.3$

Fig. 7 Upper bound model composed of lines of velocity discontinuity

3. 2 Case of Different Yield Stress for Inclusion and Matrix

Next, deformation behaviour is examined for the cases that the yield stress of the inclusion is higher (α_I = 2.0) and lower (α_I = 0.5) than that of the matrix. (Hereafter, we call the two cases as the case of hard inclusion and that of soft inclusion, respectively.) The yield stress of the boundary region is assumed to be a half of the lower value of the yield stress between the inclusion and the matrix.

Figures 8 and 9 show the distribution of the equivalent plastic strain for the hard and the soft inclusions, respectively. When the yield stress of the inclusion is higher than that of the matrix and the shape of the inclusion is isotropic (R = 1), the inclusion hardly deforms, while severe boundary slip and non-uniform deformation occurs in the matrix. Meanwhile, if the aspect ratio of the inclusion becomes larger or smaller than 1, both the inclusion and the matrix deform, and hence the boundary slip decreases. For the case of soft inclusion, deformation band appears in the OC direction for

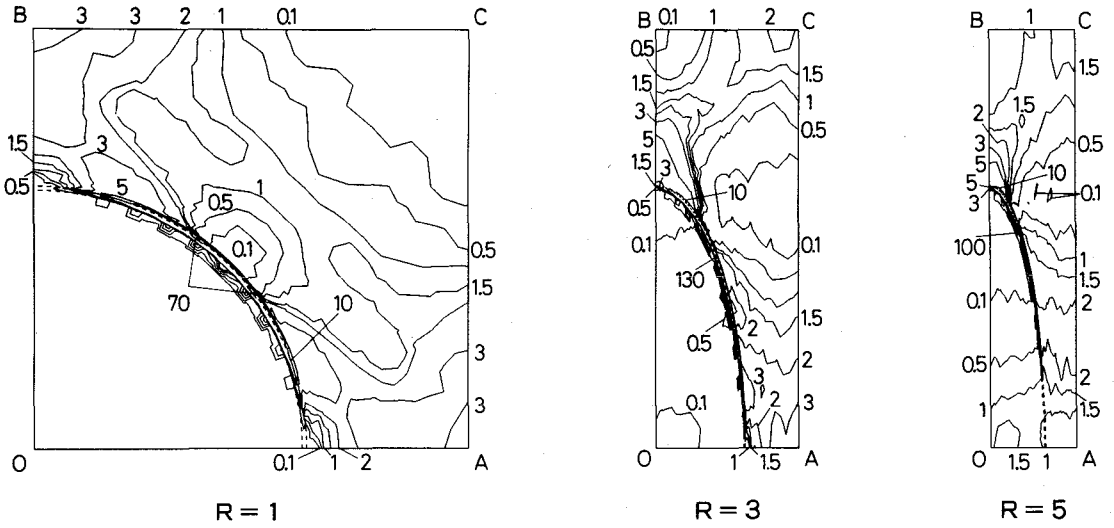

(a) $(V_f)_I$ = 0.3

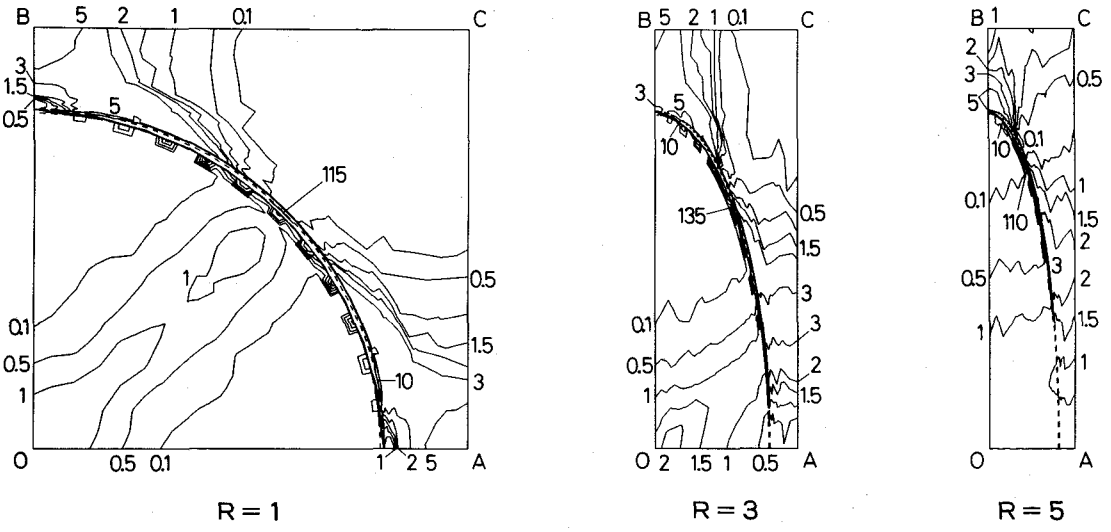

(b) $(V_f)_I$ = 0.5

Fig. 8 Distribution of equivalent plastic strain ε_{eq}
[Hard inclusion, α_I = 2.0 , α_B = 0.5 , unit : ε_x]

the aspect ratio R = 1, while deformation is relatively uniform in the matrix when R is large. The effect of the boundary slip on the non-uniform strain distribution or the formation of deformation bands is relatively small for the soft inclusion.

When Figs. 8 and 9 are compared with the former results of the distribution of the equivalent plastic strain without boundary slip[9], the effect of boundary slip between the inclusion and the matrix on deformation is marked for the case of hard inclusion, as compared with that for the case of soft inclusion.

Figure 10 shows the relation between the strain concentration coefficients A_I, A_B, A_M and the aspect ratio R, calculated from the distribution of the equivalent plastic strain and Eq. (14). For the hard inclusion, A_I shown in Fig. 10 (a) is smaller than A_M and reduces to 0 for $R \leq 2$, which shows the inclusion scarcely deforms. A_I is close to 1 for $R > 2$, that is, the inclusion as well as the matrix deform and the deformation behaviour of the whole material tends to be uniform.

For the soft inclusion, A_I is greater than A_M as is shown in Fig. 10 (c), though both A_I and A_M come close to 1 as the aspect ratio deviates from R = 1. The values of A_I and A_M decrease at R = 2 for $(V_f)_I$ = 0.2 or at R = 3 for $(V_f)_I$ = 0.3, while A_B shown in Fig. 10 (d) takes the maximum value at the same position.

Figures 11(a) and (b) shows the relation between the ratio σ^*/σ_M of the calculated averaged flow stress for the whole

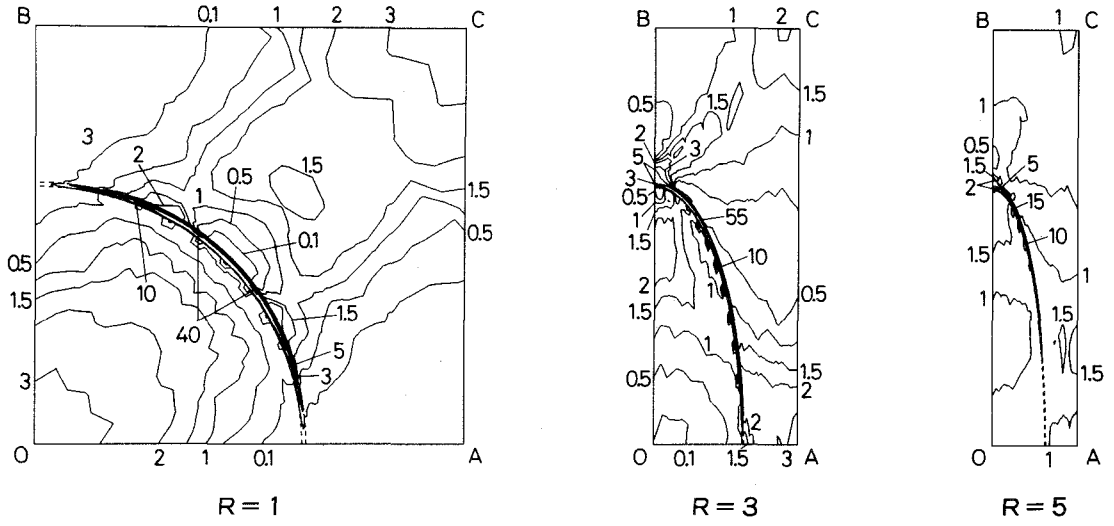

(a) $(V_f)_I$ = 0.3

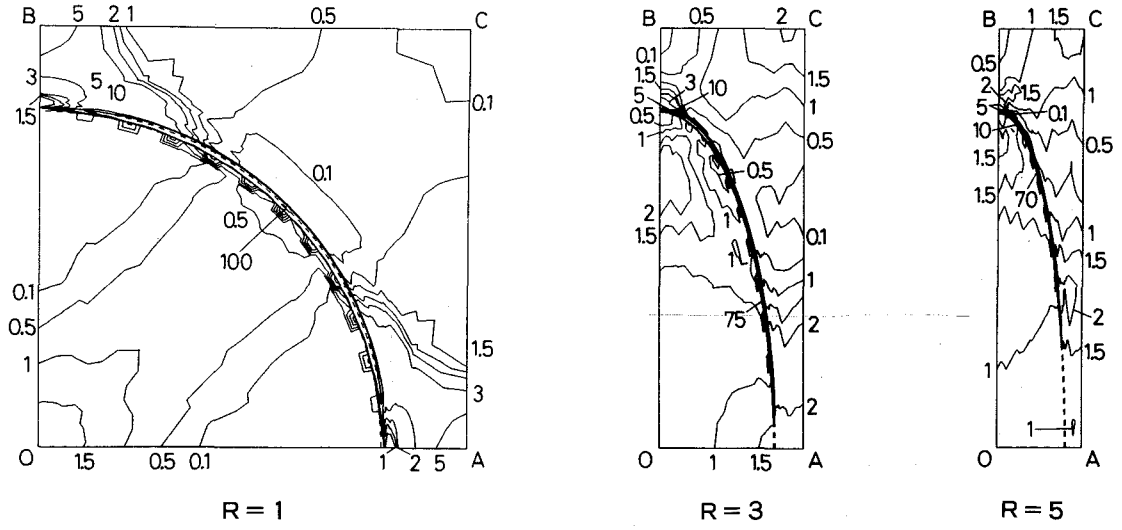

(b) $(V_f)_I$ = 0.5

Fig. 9 Distribution of equivalent plastic strain ε_{eq}
[Soft inclusion, α_I = 0.5 , α_B = 0.25 , unit : ε_x]

material to the yield stress of the matrix and the aspect ratio R. The alternate dot and dashed line shows the estimated value from the law of mixture [Eq. (19)].

When the aspect ratio R of the inclusion is larger than 10 or smaller than 0.1, the deformation is almost uniform and the averaged flow stress of the inhomogeneous material agrees with that predicted from the law of mixture. Meanwhile, when the shape of the inclusion is spherical ($R \fallingdotseq 1$), the averaged flow stress is lower than that predicted from the law of mixture. This tendency results from the non-uniform deformation and the formation of deformation bands.

Figures 12 (a) and (b) show the effect of the volume fraction of the inclusion on the averaged flow stress for the cases of the hard and the soft inclusions, respectively.

When the calculated results for the hard inclusion with boundary slip are compared with the previous ones without boundary slip[9], it follows that the flow stress σ^*/σ_M decreases with boundary slip when R is close to 1. Meanwhile, the effect of the boundary slip is less for the soft inclusion.

Figure 13 (a) shows the effect of the thickness of the boundary region on the strain concentration coefficients A_I, A_M and A_B. Fig. 13 (b) shows the effect of the thickness on the averaged flow stress. It is seen that the effect of the thickness of the boundary region on the deformation mode is relatively small.

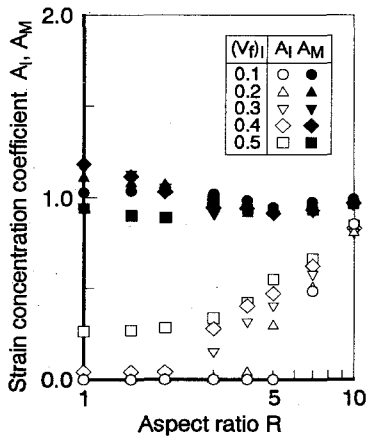

(a) A_I and A_M ($\alpha_I = 2.0$, $\alpha_B = 0.5$)

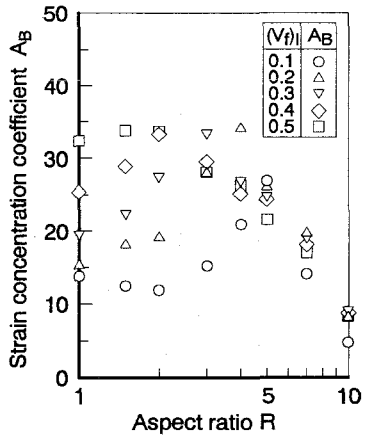

(b) A_B ($\alpha_I = 2.0$, $\alpha_B = 0.5$)

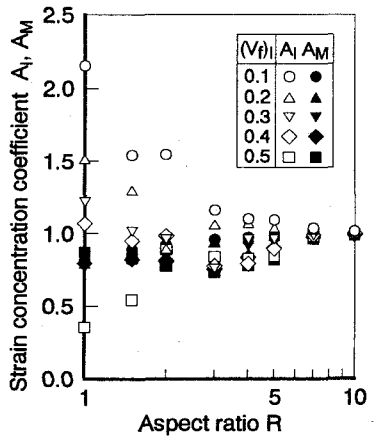

(c) A_I and A_M ($\alpha_I = 0.5$, $\alpha_B = 0.25$)

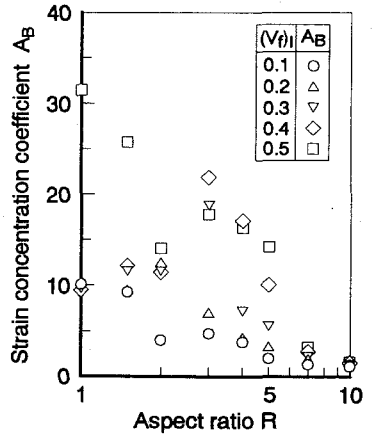

(d) A_B ($\alpha_I = 0.5$, $\alpha_B = 0.25$)

Fig. 10 Relation between strain concentration coefficients A_I, A_M, A_B and aspect ratio R

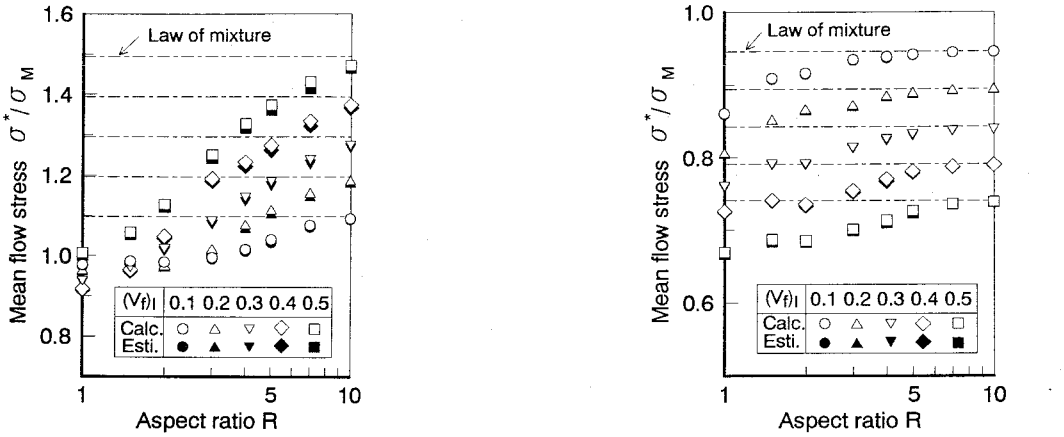

(a) Hard inclusion ($\alpha_I = 2.0$, $\alpha_B = 0.5$) (b) Soft inclusion ($\alpha_I = 0.5$, $\alpha_B = 0.25$)

Fig. 11 Relation between averaged flow stress σ^*/σ_M and aspect ratio R

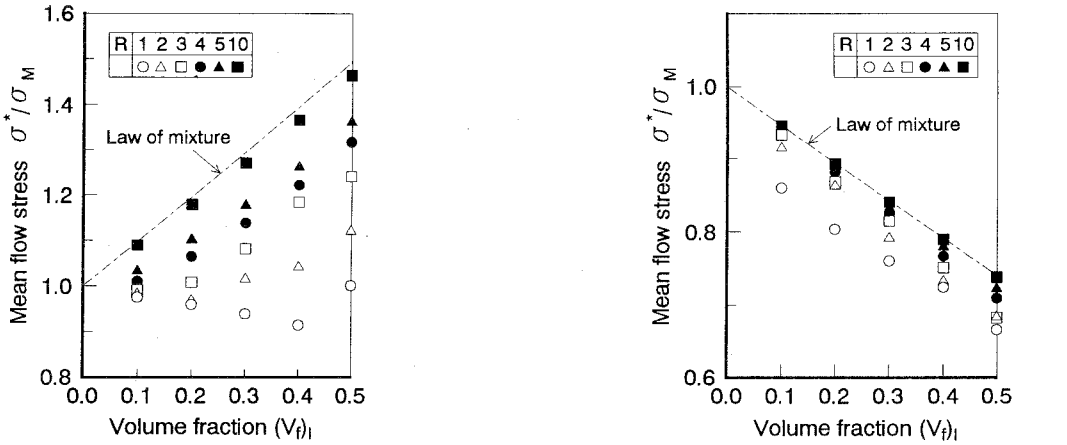

(a) Hard inclusion ($\alpha_I = 2.0$, $\alpha_B = 0.5$) (b) Soft inclusion ($\alpha_I = 0.5$, $\alpha_B = 0.25$)

Fig. 12 Relation between averaged flow stress σ^*/σ_M and volume fraction $(V_f)_I$ of inclusion

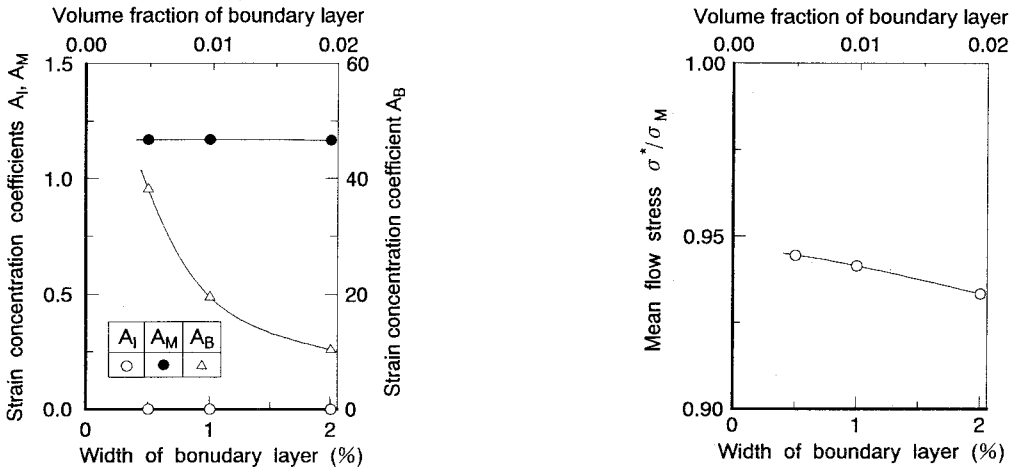

(a) Strain concentration coefficients (b) Mean flow stress

Fig. 13 Effect of thickness of boundary region [$\alpha_I = 2.0$, $\alpha_B = 0.5$, $(V_f)_I = 0.3$, $R = 1$]

4. CONCLUSION

The plastic deformation of inhomogeneous material with elliptic inclusions sliding along the boundary was studied. The model of inhomogeneous material with regularly distributed inclusions was analyzed numerically under the plane strain condition with the rigid-plastic finite element method. The influence of the yield stress of the boundary region, the aspect ratio and the volume fraction of the inclusion on the deformation behaviour, such as distribution of equivalent plastic strain, was examined. The main conclusions are summarized as follows.

(1) When the boundary region is soft and the yield stress of the inclusion and the matrix are equal, deformation bands along the boundary region appear and the non-uniform deformation increases with the decrease of the yield stress of the boundary region. This inclination is marked if the aspect ratio is close to 1, that is, when the inclusions are circular.

(2) When the yield stress of the inclusion is higher than that of the matrix, the inclusion hardly deforms for the aspect ratio close to 1, and non-uniform deformation appears in the matrix together with severe boundary slip. When the aspect ratio is much greater than 1 or smaller than 1, the inclusion deforms and the slip along the boundary decreases, which is due to mutual constraint of deformation between the inclusion and the matrix.

(3) When the yield stress of the inclusion is lower than that of the matrix, the boundary slip has little effect on the formation of deformation bands and the non-uniform distribution of strain.

(4) The deformation is almost uniform and the averaged flow stress of inhomogeneous material is close to that obtained from the law of mixture of composite materials when the aspect ratio is greater than 10 or smaller than 0.1. Meanwhile, if the aspect ratio is close to 1, the flow stress is less than that estimated from the law of mixture, which results from the non-uniform deformation accompanied with deformation bands. These results may be useful for understanding creep or superplastic deformation observed in certain alloys with inclusions.

(5) The calculated flow stress of the inhomogeneous material is also less than the upper bound estimation based on the velocity discontinuity lines along the boundary.

REFERENCES

(1) M.F. Ashby, Strengthening Methods in Crystals (ed. by A. Kelly and R.B. Nicholson), Applied Science, (1971) 137.

(2) R.J. Asaro and D.M. Barnett, J. Mech. Phys. Solids, **23**, (1975) 77.

(3) B. Avitzur, Trans.ASME, Ser.B, J. Eng. Ind., **95** (1973) 827.

(4) Y. Tada, M. Oyane, S. Shima, T. Sato and M. Omura, Trans. ASME, Ser.B, J. Eng. Ind., **105** (1983), 39.

(5) F. Ghahremani, Int. J. Solids Structures, **16**, 9 (1980) 825.

(6) T. Mori and T. Mura, J. Mech. Phys. Solids, **35**, 5 (1987) 631.

(7) T. Abe, S. Nagaki and T. Hayashi, Bulletin of JSME, 29, 255 (1986) 2797.

(8) N. Nagayama, T. Abe and S. Nagaki, Strength of Metals and Alloys (ICSMA 8) (ed. by Kettunen,P.O. et al), Pergamon (1988) 489.

(9) N. Nagayama, T. Abe and S. Nagaki, Computational Mechanics, **4** (1989) 433.

(10) T. Abe, T. Takaoka, N. Nagayama and Y. Takano, Residual Stresses-Ⅲ, Science and Technology (ed. by H. Fujiwara et al) 1201, Elsevier (1991).

(11) W. Yang and W.B. Lee, Meso-plasticity and its Applications, Springer (1992).

(12) M. Oyane and H. Sekiguchi, J. Japan Inst. Metals., **32**, 11 (1968) 1068 (in Japanese).

(13) J.D. Eshelby, Proc. Roy. Soc., Ser.A, **241** (1957) 376.

(14) T. Mura, Micromechanics of Defects in Solids, Martinus Nijihoff (1982).

(15) T. Mura and R. Furuhashi, Trans. ASME, J. Appl. Mech., **51** (1984) 308.

(16) I. Jasiuk, E. Tsuchida and T. Mura, Int. J. Solids Structures, **23**, 10 (1987) 1373.

(17) C.H. Lee and S. Kobayashi, Trans. ASME, J. Eng. Ind., **95** (1973) 865.

(18) I. Shimizu, K. Ohuchi and T.Sano, Preprint Spring Anuual Meeting, Jap.Soc.Tech.Plasticity (1988) 599 (in Japanese).

(19) R. Namikoshi, T. Abe and N. Nagayama, J. Soc. Mat. Sci., Japan, **42** (1993) 1065 (in Japanese).

(20) R. Hill, J. Mech. Phys. Solids, **11** (1963) 357.